The Astrophysical Journal, 497:L117–L121, 1998 April 20

HCO^+ IMAGING OF COMET HALE-BOPP (C/1995 O1)

Amy J. Lovell, F. Peter Schloerb, James E. Dickens, Christopher H. DeVries, Matthew C. Senay, and William M. Irvine
Five College Radio Astronomy Observatory, Department of Physics and Astronomy, University of Massachusetts, Amherst, MA 01003; lovell@fcrao1.phast.umass.edu
Received 1998 January 13; accepted 1998 February 17; published 1998 March 11

ABSTRACT

The HCO^+ $J = 1–0$ rotational transition at 89.189 GHz has been mapped in comet Hale-Bopp (C/1995 O1) over a total of 38 individual days spanning the period 1997 March 10–June 20 with the Five College Radio Astronomy Observatory 14 m antenna. HCO^+ is detectable over an extended region of the comet, with the peak emission commonly located 50,000–100,000 km in the antisolar direction. Maps made throughout the apparition show significant variability in the structure of the HCO^+ coma, sometimes on timescales of several hours. The HCO^+ brightness is usually depressed at the nucleus position, and on some occasions, the emission is spread into a ring around the position of the nucleus. Individual spectra within the maps display broad (approximately 4 km s^{-1}) lines redshifted by 1–2 km s^{-1} or more from the nominal velocity of the nucleus, with the redshift typically increasing in the antisolar direction. The spectra and maps may be generally explained by models in which the ions are accelerated tailward at a rate on the order of 10 cm s^{-2}, provided that HCO^+ is destroyed within 50,000–100,000 km of the nucleus.

Subject headings: comets: individual (Hale-Bopp 1995 O1) — molecular processes — plasmas — radio lines: solar system

1. INTRODUCTION

The 1997 apparition of Hale-Bopp (C/1995 O1) provided an unprecedented opportunity to study a bright comet with modern, sensitive, millimeter-wave instrumentation. Among the many new cometary detections in comet Hale-Bopp was that of the molecular ion HCO^+ through its $J = 1–0$ rotational transition at 89.189 GHz (Veal et al. 1997). The HCO^+ lines were discovered to have an overall redshift with respect to the cometocentric velocity, along with asymmetric line wings extending redward. Spectral line maps of this ion at the Five College Radio Astronomy Observatory (FCRAO), made to follow up the discovery, confirmed the redshifted line profiles and revealed an intensity distribution that was dramatically different from that of neutral molecules (Lovell et al. 1997). In this Letter, we summarize the results of a 3 month observing campaign to map HCO^+ in comet Hale-Bopp.

2. OBSERVATIONS

All observations were performed with the FCRAO 14 m radome-enclosed telescope in New Salem, Massachusetts. The HCO^+ $J = 1–0$ rotational transition at 89.189 GHz was observed in comet Hale-Bopp during a period from March 10 to June 20, which includes both perigee ($\Delta = 1.3$ AU) and perihelion ($r = 0.92$ AU).

The receiver front end was the 15 element focal-plane array (QUARRY) of cooled Schottky receivers tunable between 85 and 115 GHz (Erickson et al. 1992). The typical system temperature obtained with this receiver is 450 K single-sideband during the good weather conditions that prevailed on most observation dates. The back end used was the 1024 channel Focal-Plane Array Autocorrelating Spectrometer, which provided a maximum velocity resolution (in all 15 array pixels) of 66 m s^{-1}. All HCO^+ maps were obtained by frequency switching with a 6 MHz offset.

The position of the comet nucleus on the sky was computed and tracked using a two-body ephemeris program. The two-body orbital elements were provided by D. Yeomans of JPL and were updated regularly throughout the observations. The focal-plane array was rotated as necessary in order to align the rows of the array with the Sun-tail axis of the comet. This procedure preserves a grid of observations fixed with respect to the comet in order to facilitate data averaging. The data were obtained on a Nyquist-sampled grid, with the comet sampled by the 60″ beams of the array at 25″ intervals. Near perigee, Nyquist sampling required up to 32 individual pointings of the 15 elements of the array in order to map the emission fully. Throughout most of the observing period, the individual spectra from each day were incorporated into a daily average map by convolving them onto an oversampled 15″ grid using a 60″ Gaussian convolution function. In some cases near perihelion, average maps were constructed for a fraction of one day's observations, as discussed below.

3. RESULTS

A sampling of individual maps of the integrated HCO^+ line area are shown in Figure 1. Several features are apparent. First, in contrast to neutral species observed with the same instrumentation, the HCO^+ ion is detected over a wide spatial region, and the emission peaks in the tailward direction, rather than on the nucleus position. Figure 2 shows a comparison between maps of HCO^+ and the neutral molecule HCN (for which the observed 88.632 GHz $J = 1–0$ transition has excitation requirements similar to the $J = 1–0$ HCO^+ line) obtained on adjacent days, to illustrate the difference in extent and peak position of the emission. The ion emission is detected over an area approximately 4 times that of the neutral emission, and its peak emission is obviously shifted antisunward.

It is also apparent from Figure 1 that the HCO^+ emission is time-variable. In particular, we note that the two panels from 1997 April 3, the first pretransit and the second posttransit, demonstrate that the character of the mapped emission can change on timescales of less than 4 hr. Significant intensity changes also occur between maps on adjacent observing days,

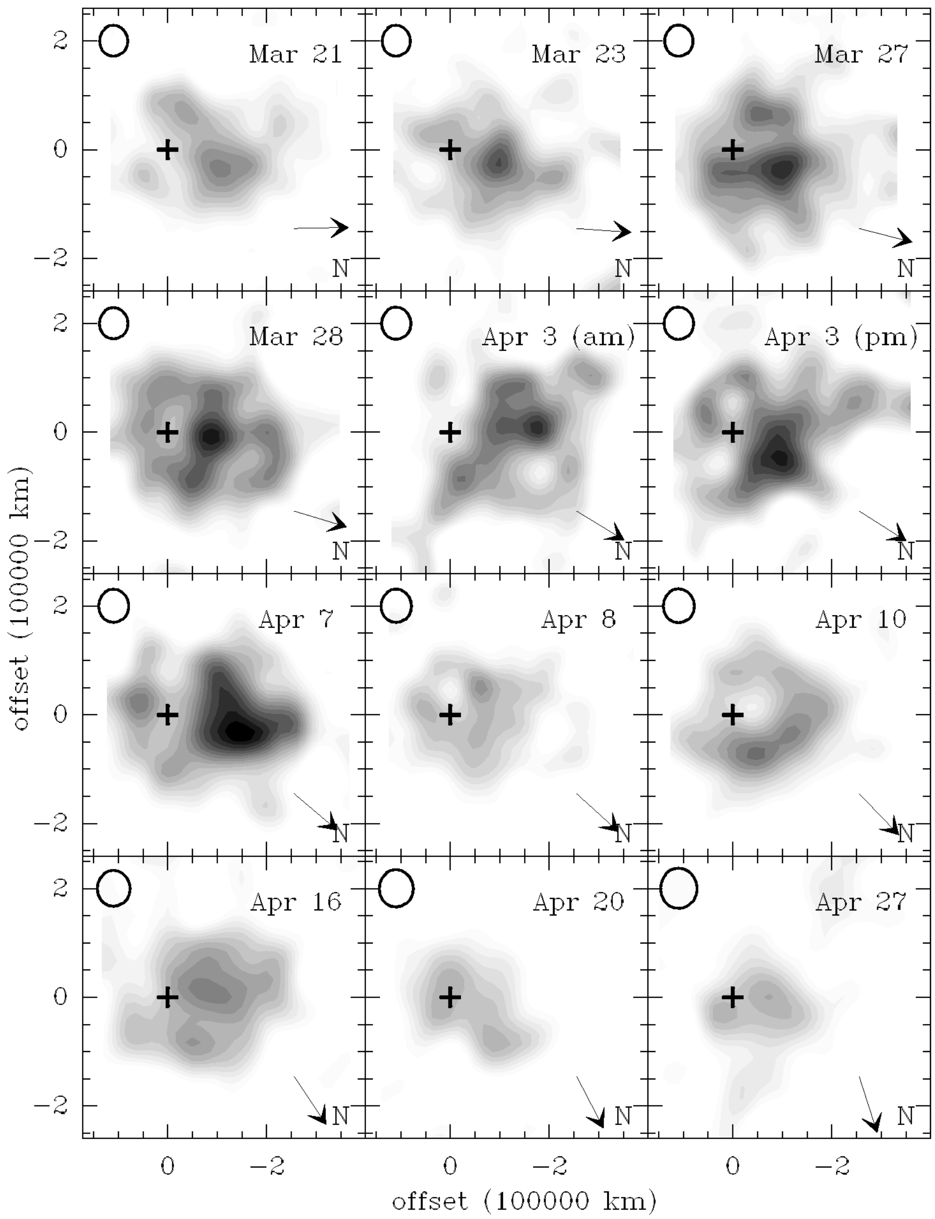

FIG. 1.—A sampling of maps of the HCO^+-integrated intensity in comet Hale-Bopp at heliocentric distances less than or equal to 1 AU. The Sun is to the left (positive *x*) in all images, with north in the direction of the arrow. Due to the changing geocentric distance, the physical size of the 1′ beam changes as indicated by the circle. The contour interval is 33 mK km s^{-1}, beginning at 100 mK km s^{-1}. Note the offset in the emission peak away from the nucleus (at the cross) and the appearance of a "ring" structure in some maps.

as is nicely illustrated by the maps of April 7 and 8. These two maps also demonstrate two distinctive morphologies that are apparent in the HCO^+ emission: a single strong peak that is displaced antisunward and more diffuse emission spread out into a ring or horseshoe shape, with a local minimum on the nucleus position.

In order to evaluate the typical behavior of HCO^+ emission from the comet, we have averaged 8 individual days, between 1997 March 23 and April 10, to improve the signal-to-noise ratio in the spectra. Results derived from this averaged data set are shown in Figure 3. The left panel shows a map of the integrated intensity of the spectral lines. Individual spectra along the solar-antisolar axis are shown in the right panel of the figure. The spectral line emission in the average map follows the basic trends identified in the maps on individual days. The HCO^+ emission is clearly stronger in the antisolar direction, and there is a depression in the map at the position of the nucleus. The HCO^+ spectral lines are broad and redshifted with respect to the nucleus velocity; the amount of the redshift increases as one observes progressively farther down the tail of the comet.

4. DISCUSSION

Once HCO^+ is formed in the coma, it should be accelerated in the antisolar direction through its interaction with the solar wind magnetic field streaming past the comet. Thus, the basic redshift of the HCO^+ lines and the asymmetric distribution of its emission are probably best accounted for by this process. A complete model of this phenomenon would involve a full MHD treatment of the interaction of the solar wind with the cometary plasma (cf. Wegmann & Schmidt 1987) but would

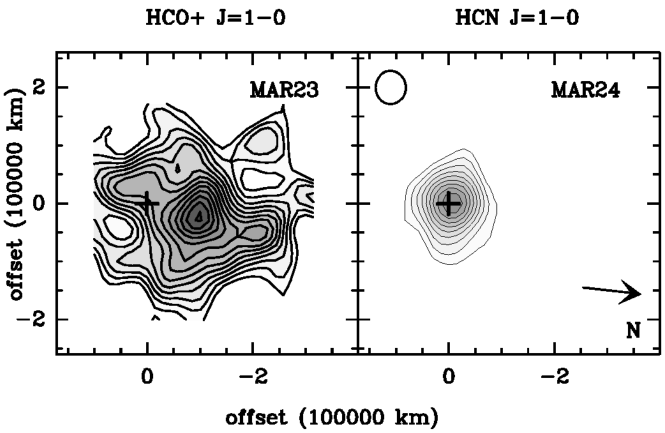

FIG. 2.—Comparison of maps of HCO$^+$ $J = 1$–0 and HCN $J = 1$–0 emission obtained on successive days (1997 March 23 and 24). Although these molecules have similar excitation requirements and are observed with the same size beam, the ion emission is observable over a larger area and offset from the nucleus position. The symbols are the same as in Fig. 1.

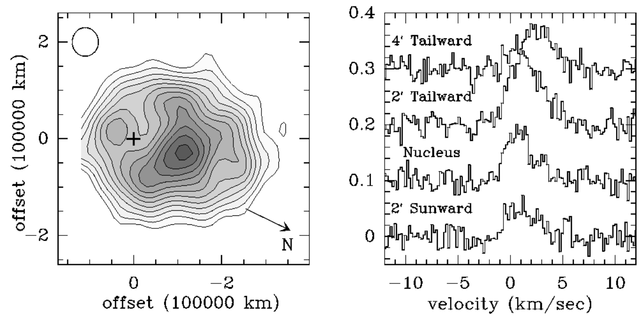

FIG. 3.—An average map of HCO$^+$ derived from data obtained on 8 days between 1997 March 23 and April 10. The left panel shows the map of integrated intensity, with a contour interval of 33 mK km s^{-1}, beginning at 100 mK km s^{-1}. The Sun is to the left of the frame, and other symbols are the same as in Figs. 1 and 2, representing the mean beam size and orientation of north. The right panel shows spectra from the averaged map obtained at four positions along the Sun-tail axis. These spectra illustrate the broad, redshifted lines of HCO$^+$ and the variation in redshift along the comet tail.

be beyond the scope of this Letter. We have, therefore, adopted a simple model in which ions are formed and then accelerated tailward with a fixed acceleration. This approximation allows a quantitative analysis of our maps.

HCO$^+$ ions could be formed in a cometary coma through a number of paths. The most likely scenario is the formation of HCO$^+$ via ion-molecule reactions. CO is first photoionized to give CO$^+$, which then reacts with water to produce HCO$^+$ (Huebner & Giguere 1980). Given the results of Huebner & Giguere's models and our present understanding that H_2O and CO are the most abundant molecules in the comet's coma, this path is the most plausible, and we have adopted it for our model simulation. On formation, HCO$^+$ may be photodestroyed, destroyed by reactions with neutrals, or lost through recombination with electrons.

For the purpose of our simple model, we adopt the above formation scheme and specify (1) the lifetime of CO against photoionization, (2) the lifetime for CO$^+$ against reaction with water in the coma as a function of distance from the nucleus, and (3) a lifetime for HCO$^+$ against destruction by all processes. For CO photoionization, we adopt a quiet-Sun lifetime of 3×10^6 s at a heliocentric distance of 1 AU (Schmidt et al. 1988). The lifetime of a CO$^+$ ion due to reaction with H_2O is deduced from the rate constant (k), which should be variable within the coma since the water density decreases in proportion to the inverse square of the distance from the nucleus. We adopt a gas production rate (Q) of 10^{31} s^{-1} for the comet and a water outflow velocity (v) of 1 km s^{-1} to derive the reaction timescale, τ, at distance r in the coma (reaction constants from Schmidt et al. 1988):

$$\tau(r) = \frac{1}{k}\frac{4\pi v r^2}{Q} = 1.4 \times 10^4 \left[\frac{r\,(\mathrm{km})}{10^5}\right]^2 . \qquad (1)$$

The destruction of HCO$^+$ ions is obviously critical to the interpretation of the HCO$^+$ maps. Our initial assumption for this work has been to adopt a single lifetime for HCO$^+$ destruction and examine the consequences for a range from long values, which would be appropriate to photodestruction, to very short values, which might pertain to recombination in the inner coma.

We have computed the effects of both the HCO$^+$ formation and its acceleration using a Monte Carlo approach (cf. Tacconi-Garman, Schloerb, & Claussen 1990). This technique is essentially a simulation of the formation and kinematics of HCO$^+$, followed by a line-of-sight integration of the numbers of molecules and their velocities to compute the model spatial distribution and spectra. The left panel of Figure 4 shows the results of model computations, assuming a tailward acceleration of 10 cm s^{-2} and a relatively long lifetime of 10^5 s for HCO$^+$ after its formation. Qualitatively, the model shows the general features of a large, asymmetric brightness distribution

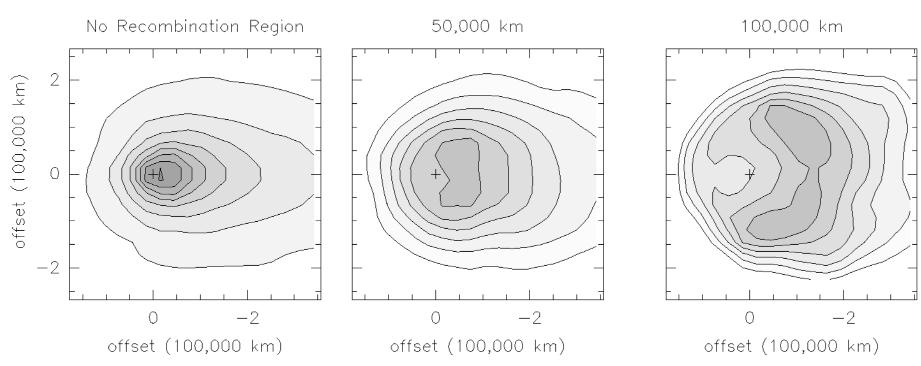

FIG. 4.—Model maps of HCO$^+$-integrated intensity in comet Hale-Bopp, using a value of 10 cm s^{-2} for acceleration. The left image has no recombination region, the center image includes recombination inside a radius of 50,000 km, and the right image includes recombination inside a radius of 100,000 km.

for HCO^+, and model spectral lines show the redshifted behavior that is observed. Quantitatively, a simpler approach is to compare the mean velocity of spectra along different lines of sight in the coma. In Figure 5, we show a comparison of the mean velocity of model spectra with the observed mean velocity derived from the averaged map of Figure 3. Model predictions for an acceleration of 5, 10, and 20 cm s^{-2} are presented (*solid lines*), and the comparison with the actual measurements suggests that an acceleration on the order of 10 cm s^{-2} is sufficient to explain the magnitude of the redshift and its variation in the coma. This value is about a factor of 10 smaller than values derived from observations of the tail of comet Halley by Celnik & Schmidt-Kaler (1987) and Scherb et al. (1990), presumably because of the increase in mass loading of the solar wind in this high production rate comet. In addition, the velocity within the map appears to require greater values of acceleration as ions proceed along the tail (Fig. 5).

Although the left panel of Figure 4 shows the basic asymmetry seen in our maps, the peak emission in this model is not offset from the nucleus position by the amount that is typically observed. Moreover, this model cannot reproduce the local minimum on the maps that is strongly suggested by the "ring" features that are observed on some days. Thus, we have attempted to refine the basic model in order to achieve better agreement with the maps. We consider a region within the inner coma where recombination of HCO^+ and CO^+ occurs at a high rate. Such a model is consistent with the observed behavior of comet Halley, where Eberhardt & Krankowsky (1995) found a large increase in the electron recombination rate for ions in the inner coma at a distance of about 5000–10,000 km from the nucleus. The discontinuity in comet Halley occurs outside of the contact surface and corresponds to the point in the coma where cooling of electrons through collisions with neutrals becomes ineffective. Since the contact surface radius should scale with the comet's production rate (Ip & Axford 1990), we expect that the effect seen in comet Halley should occur approximately 10 times farther out in Hale-Bopp, or at approximately 50,000–100,000 km from the nucleus.

Figure 4 shows calculations that assume that HCO^+ cannot survive within 50,000 km (*center panel*) and 100,000 km (*right panel*) of the nucleus. The maps that include a recombination region display not only the offset in the peak of the HCO^+ emission but also the "ring" behavior that is observed. Thus, we conclude that the appearance of the observed HCO^+ maps requires the existence of such a region. Additional evidence in favor of a large recombination region is seen in the dotted curves of Figure 5, which show the predicted mean velocity of lines in the presence of a 50,000 km recombination region. The disappearance of HCO^+ molecules from the inner coma in these models primarily affects molecules at low velocities near the nucleus. The result is that the mean velocity toward the nucleus position is greater than that observed in models with no recombination region. The predicted variation of mean velocity with position in the coma is in good agreement with the observed behavior of the comet and appears to confirm our conclusion that the appearance of the maps is the result of missing HCO^+ ions in the inner coma.

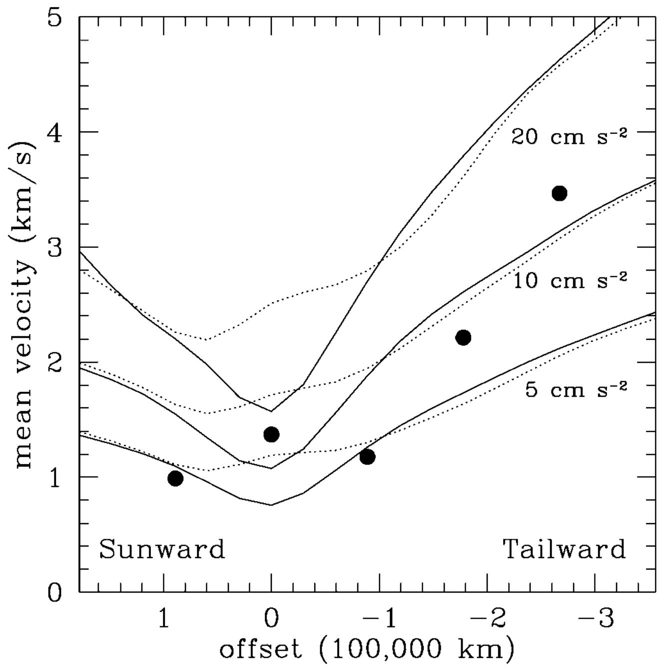

FIG. 5.—Mean velocity of spectral lines along the Sun-tail axis of the comet. The data (*filled circles*) are derived from the averaged map of Fig. 3. The solid lines show the result of models that consider only acceleration of the ions. The dotted lines illustrate models that include a 50,000 km recombination region. Note that the models that include recombination better reproduce the observed behavior of the comet.

5. CONCLUSIONS

We have mapped the HCO^+ emission from comet Hale-Bopp and identified several key aspects of its behavior. The HCO^+ emission is extended tailward, and it is significantly redshifted compared with neutral species. Maps on many days illustrate that the HCO^+ emission is significantly time variable to the shortest timescales that we were able to probe (several hours).

The general features of the HCO^+ emission may be understood by a simple model in which its formation is followed by acceleration via interaction with the solar wind magnetic field. The acceleration of the ions accounts for the basic asymmetry in the emission and for the observed redshifts of the lines. However, the maps also appear to require a region of enhanced HCO^+ destruction within approximately 50,000–100,000 km of the nucleus. The scale of this region corresponds quantitatively to a region of enhanced recombination in the inner coma of comet Halley, as observed by instruments on the *Giotto* spacecraft (cf. Eberhardt & Krankowsky 1995). This region occurs at an important transition in the coma between gas that is dominated by cold cometary species and gas in which solar wind and cometary ions are being mixed. Thus, given the time variability of both the solar wind and the gas production from the comet, it is not surprising to find significant time variability in the behavior of the HCO^+ emission.

The authors acknowledge thought-provoking conversations about ion-molecule chemistry in comets with E. A. Bergin. Planetary astronomy at the University of Massachusetts is supported by NASA grants NAGW-1483 and NAG5-4743. Astronomical research at the FCRAO is supported by the NSF under grant AST-9420159. The authors also acknowledge NSF funding under a special Hale-Bopp opportunity grant AST-9615610 to the University of Massachusetts.

REFERENCES

Celnik, W. E., & Schmidt-Kaler, Th. 1987, A&A, 187, 233
Eberhardt, P., & Krankowsky, D. 1995, A&A, 295, 795
Erickson, N. R., Goldsmith, P. F., Novak, G., Grosslein, R. M., Viscuso, P. J., Erickson, R. B., & Predmore, C. R. 1992, IEEE Trans. Microwave Theory Tech., MTT-40, 1
Huebner, W. F., & Giguere, P. T. 1980, ApJ, 238, 753
Ip, W.-H., & Axford, W. I. 1990, in The Physics and Chemistry of Comets, ed. W. F. Huebner (Berlin: Springer), 199
Lovell, A., Schloerb, P., DeVries, C., Dickens, J., Irvine, W., & Senay, M. 1997, IAU Circ. 6590
Scherb, F., Magee-Sauer, K., Roesler, F. L., & Harlander, J. 1990, Icarus, 88, 172
Schmidt, H. U., Wegmann, R., Huebner, W. F., & Boice, D. C. 1988, Comput. Phys. Commun., 49, 17
Tacconi-Garman, L. E., Schloerb, F. P., & Claussen, M. J. 1990, ApJ, 364, 672
Veal, J. M., et al. 1997, IAU Circ. 6575
Wegmann, R., & Schmidt, H. U. 1987, A&A, 187, 339